

and outside this cylinder ($r \geq R$)

$$E_z^{\text{out}} = \beta_0^+ \tilde{H}_0 + 2 \sum_{k>0} \beta_k^+ \tilde{H}_k \cos(k\phi) + 2i \sum_{k>0} \beta_k^- \tilde{H}_k \sin(k\phi) \quad (2)$$

with

$$\tilde{J}_k(r) = J_k(2\pi r n / \lambda) \quad \text{and} \quad \tilde{H}_k(r) = \frac{H_k(2\pi r / \lambda)}{H'_k(2\pi R / \lambda)}. \quad (3)$$

Here $J_k(r)$ are Bessel functions and $H_k(r)$ are Hankel functions of the first kind [23]. Note that Hankel functions are normalized by a factor $H'_k(2\pi R / \lambda)$ in order to eliminate numerical instabilities caused by very large values of Hankel functions of small arguments. The angle ϕ is defined in Fig. 1. The EM field in the vacuum has a wavelength $\lambda = 2\pi / \omega$ and $n = \sqrt{\epsilon\mu}$ is the refractive index of material of cylinder.

The field E_z scattered by other cylinders centered at $\vec{r} = (n_x a, n_y a)$ can be expressed in the form of Eqs. (1) and (2) with a new set of coefficients $\alpha(n_x, n_y)$ and $\beta(n_x, n_y)$ and cylindrical coordinates r and ϕ corresponding to the position of each cylinder.

Two components of magnetic fields, H_r and H_ϕ , will be calculated from Maxwell's equations:

$$H_r = -\frac{i}{\omega\mu r} \frac{\partial E_z}{\partial \phi}, \quad H_\phi = \frac{i}{\omega\mu} \frac{\partial E_z}{\partial r}. \quad (4)$$

Requirements of continuity of tangential components of electric and magnetic fields at the interfaces of each cylinder give us a system of linear equations for coefficients α and β . This system can be considerably simplified in three steps: First, we can express all fields associated with various cylinders in terms of variables r and ϕ associated with the cylinder located at the point $x = 0$, $y = 0$. This can be done with the use of the transformation formula for cylinder functions [23]

$$\mathcal{C}_m(w) e^{\pm imx} = \sum_{k=-\infty}^{+\infty} \mathcal{C}_{m+k}(u) J_k(v) e^{\pm ik\alpha} \quad (5)$$

for $\mathcal{C}_m = H_m$ and its derivative (See Fig. 2 for definition used symbols). Second, since the structure is periodic in the x direction we use the Bloch theorem

$$\alpha(n_x, n_y) = \alpha(0, n_y) e^{ik_x a n_x}, \quad (6)$$

$$\beta(n_x, n_y) = \beta(0, n_y) e^{ik_x a n_x}, \quad (7)$$

to reduce considerably the number of unknown parameters. Third, coefficients α could be easily expressed as

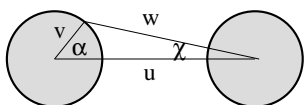


FIG. 2: Parameters used in equations (5).

a linear combination of coefficients β . Finally, if N_B is the highest order of the Bessel function used in Eqs. (1) and (2), we end up with $N \times (2N_B + 1)$ linear equations for unknown coefficients $\beta_k^\pm(n_y)$ ($k = 0, 1, \dots, N_B$, $n_y = 0, 1, \dots, N - 1$)

$$\mathbf{C}\beta = \mathbf{f}. \quad (8)$$

The vector \mathbf{f} the right hand side of Eq. (8) defines an incident EM wave.

In numerical simulations, we use typically $N_B = 12$. Then, in the case of linear array of cylinders, the program solves for each frequency the system of $2N_B + 1 = 25$ linear equations. For the photonic slab composed from $N = 24$ chains, the number of equations increases to 600. The central point of the algorithm is the calculation of elements of the matrix \mathbf{C} in Eq. 8. This task requires summation of contributions of field scattered on all cylinders in the structure. Explicit form of matrix \mathbf{C} is given elsewhere [17]. We consider $N_x \sim 10^4$ cylinders along the x axis.

The transmission coefficient can be calculated as a ratio $T = S/S^i$ of Poynting vectors calculated on the opposite side of the structure to the incident Poynting vector S^i .

For a given frequency f , we obtain all coefficients $\beta(0, n_y)$. Assuming that

$$\beta(0, n_y) = \beta(0, 0) e^{iq a n_y} \quad (9)$$

we find the wave vector q of the EM wave propagating through the structure and, consequently, calculate the band spectrum of the two-dimensional array of cylinders [11, 16].

III. FANO RESONANCES IN VARIOUS PHOTONIC STRUCTURES

Numerical algorithm described in Section II can be used for the calculation of the frequency dependence of the transmission and reflection coefficient of any periodic structure composed from parallel cylinders. For the systems of $N = 24$ rows of cylinders, considered in this paper, we expect that, owing to spatial periodicity, the frequency dependence of transmission coefficient would exhibit a series of Bragg transmission bands separated by gaps [12, 13]. This idyllic picture is disturbed by excitation of Fano resonances [3, 11]. While the eigenfrequency of Fano resonance is determined by the material parameters and shape of individual cylinder, the position of Bragg band is given by the spatial periodicity of the structure. Two bands of different origin – Bragg and Fano – can therefore overlap. Interference of two bands strongly influences resulting frequency bands observed in the spectrum. For instance, we will see below that Fano resonance can split an original Bragg band into two separated bands. For the qualitative understanding of frequency spectra and identification of the origin of

individual frequency bands is useful to calculate the frequency dependence of all parameters α and β defined in Eqs. (1,2) and determine the order n of Fano resonances from their resonant behavior.

We identify resonances excited in three photonic structures. We start with isolated cylinder [21, 22, 24]. The second structure of interest is a linear chain of cylinders. We show that each resonance excited in the cylinder is splitted into two resonances – even and odd – when incident wave scatters on an infinite array of cylinders. The third structure consists from $N = 24$ linear rows of cylinders. If resonances observed in the linear chain, do not couple with Bragg transmission bands, they develop into separated transmission bands. Typically, these bands are very narrow (their width is determined by the overlap of fields excited at neighboring cylinders).

A. Dielectric cylinders with high permittivity

Periodic array of dielectric rods have been analyzed in [10]. In our work [11] we studied the formation of Fano bands and interaction between Bragg and Fano bands. in the array of dielectric cylinders of radius $R = 0.4a$ and permittivity $\varepsilon = 12$ and found five Fano bands in the frequency interval $f = a/\lambda < 1$. The number of resonances increases when either cylinder radius [11] or the permittivity increases. While the increase of the radius is limited by the spatial period of the structure, the permittivity can possess, at least in theoretical model, rather high values. In this paper, we study dielectric cylinders of radius $R = 0.4a$ and permittivity $\varepsilon = 80$. Incident EM wave is polarized with E_z parallel to cylinders. Results are summarized in Figs. 3 and 4.

Left Fig. 3 shows the spectrum of resonances excited on an isolated cylinder. A series of resonances for each coefficient α_n corresponds to oscillation of Bessel function J_n inside the cylinder [22]. Right Fig. 3 shows how Fano resonances influence the transmission coefficient of plane wave propagating through linear chain of dielectric rods. For the sake of simplicity, the incident angle $\theta = 0$ so that only even resonances are excited [25]. Besides Fabry-Perot oscillations of transmission coefficient we identify irregularities in transmission when frequency of incident wave coincides with the eigenmode of the structure [3]. To demonstrate the creation of Fano transmission bands, we add in panel (d) also the transmission coefficient for the finite photonic slab.

Spatial distribution of electric field for a few selected resonances is shown in Fig 4. The order n of resonance is clearly visible, and can be confirmed by the frequency dependence of coefficients α_{2k}^+ and α_{2k-1}^- (not shown). Since EM wave propagates along the y axis (from the left to the right), all excited resonances are even ($E_z(-x) = E_z(x)$). Frequency $f = 0.28025$ corresponds to the first resonance of the 4th order. At frequency $f = 0.3075875$ the second resonance of α_2^+ is excited. Two resonances of the 5th order, excited at fre-

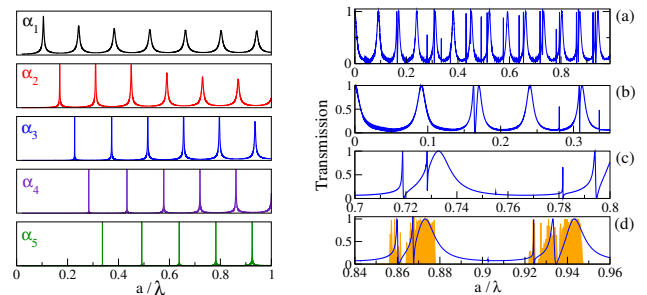


FIG. 3: Left figure: Resonances of coefficients α_n , $n = 1 - 5$ excited on isolated dielectric cylinder with permittivity $\varepsilon = 80$ and radius $R = 0.4a$. EM wave is E_z -polarized. Right figure: (a) Transmission of E_z -polarized plane wave through a linear chain of dielectric cylinders. Panels (b-c) show detailed frequency dependencies in three intervals. Panel (d) shows also the transmission coefficient for an array of $N = 24$ rows in two resonant frequency regions (shaded line). Incident angle $\theta = 0$ so that only even resonances are excited [25].

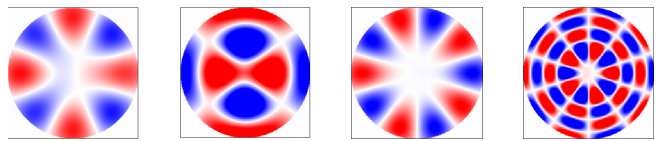


FIG. 4: Electric intensity E_z inside the cylinder for four selected resonant frequencies $a/\lambda = 0.28025, 0.307875, 0.33542$ and 0.7815 in linear cylinder chain. Note that incident plane EM wave propagates along the y direction.

quencies $f = 0.33542$ and 0.7815 , correspond to the 1st and the 4th resonance of α_5^- , respectively. (Note that in accordance with notation used in Eq. (1), resonances of α_{2k}^+ and α_{2k-1}^- are even, while resonances of α_{2k}^- and α_{2k-1}^+ are odd with $E_z(-x) = -E_z(x)$.)

B. Thin metallic rods

Frequency spectrum of periodic arrays of metallic rods has been investigated in [14, 15] and recently in [16]. It has been shown that Fano resonances could be associated with surface waves excited at the interface between cylinder and embedding media. To observe them, we consider the incident wave polarized with magnetic intensity H_z parallel to the cylinders.

We analyze resonant behavior of periodic arrays of thin metallic rods of radius $R = 0.1a$. The permittivity of metal is given by Drude formula with plasma frequency $f_p = 1$

$$\varepsilon_m = 1 - \frac{\lambda^2}{a^2} \quad (10)$$

so that the wavelength corresponding to f_p equals to the spatial periodicity a .

Owing to dispersion relation of surface waves [26, 27], we expect a series of Fano bands in narrow frequency interval below the frequency $\sqrt{2}/2$.

Figure 5 shows the resonances of coefficients α for isolated metallic cylinder. Resonant frequencies f_n converge to the limiting value $\sqrt{2}/2$ when $n \gg 1$. This confirms that Fano resonances are associated with an excitation of surface waves. The n th resonance is excited when the wavelength Λ of surface wave fulfills the relation $n\Lambda = 2\pi R$. With the use of the dispersion relation for surface waves,

$$\Lambda = \lambda \sqrt{\frac{\varepsilon}{\varepsilon + 1}} \quad (11)$$

it is easy to verify that observed resonant frequencies are identical with frequencies found from Eq. (11).

The band spectrum of periodic array of thin metallic cylinders is shown in Fig. 6(a). Since all Fano resonances are concentrated in a narrow frequency interval $0.69 < f < 0.707$, it seems, on the eye, that three broad frequency bands shown in Fig. 6(a) are periodic Bragg bands. However, since both the 2nd and the 3rd bands have a minimum in the X point, we suppose that they originate from one Bragg band which is splitted into two bands by Fano resonances. Similar split of Bragg band has been described in dielectric photonic crystal in Ref. [11]. To support this conjecture, we shown in Fig. 6(a) the frequency spectrum of periodic array of cylinders with positive dispersive permittivity $\varepsilon(f) = -\varepsilon_m(f)$. Now, since the permittivity is positive, no surface modes could be excited and we indeed observe an unperturbed 2nd band for $f > 0.5$.

In the gap between two splitted Bragg bands, $0.67 < f < 0.71$, we observe a series of very narrow Fano bands. Their frequency can be estimated approximately from resonances shown in Fig. 5. As an example, we show in Figure 6(d) the 2nd Fano band associated with the resonance of coefficient α_2^+ lying in the interval $0.6935 < f < 0.6960$. Very narrow 3rd band is also identified at frequency ~ 0.7026 . The width of higher Fano resonances decreases rapidly. For instance, the width of the 5th Fano bands located at $f = 0.70564832$ is only $\sim 10^{-7}$. We have no ambition to analyze all these frequency bands numerically, only show in Fig. 7 the distribution of magnetic intensity H_z calculated for the 5th resonance on an array of cylinders. As expected, the field is concentrated along the cylinder surfaces and is small in the center. Higher

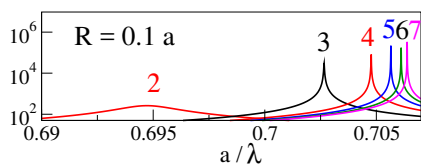


FIG. 5: Resonant behavior of parameters α_n for an isolated metallic cylinder.

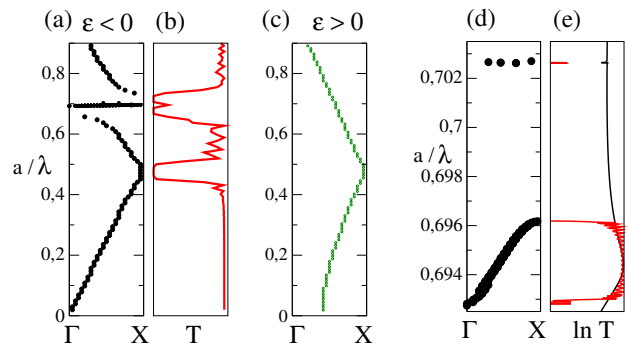


FIG. 6: (a,b) Band structure and the transmission coefficient of the photonic slab composed from $N = 24$ rows of metallic cylinders ($R = 0.1a$). (c) Frequency bands of photonic crystals composed from cylinders with positive permittivity $\varepsilon = -\varepsilon_m = a^2/\lambda^2 - 1$. (d) Two even Fano bands $n = 2$ and $n = 3$. (e) Transmission coefficient for a plane wave propagating perpendicularly through a linear chain (black line) and through $N = 24$ rows of cylinders (red line). Only even Fano bands are displayed. Odd bands are discussed in Figs. 8 and 9.

resonances at thicker metallic cylinders are discussed in [16].

Figure 8 presents the transmission coefficient for the linear chain of cylinders in the vicinity of the third cylinder resonance $f \approx 0.70266$. Figure confirms that single resonance observed at isolated cylinder splits to even and odd resonances in the linear chain of cylinders. Since each resonance corresponds to Fano band in 2D photonic crystal, we expect that Fano bands in photonic crystals appear always in pairs with even lower bands and odd higher band [16].

Of particular interest are interference effect caused by overlap of two Fano bands shown in Fig. 9. Since the even 2nd Fano band is rather broad, it overlaps over narrow odd 2nd band. This can be seen in Fig. 9(a). For zero incident angle, odd resonance does not couple to the incident wave [25] and the transmission coefficient exhibits regular frequency dependence typical for transmission band shown in Fig. 9(b). However, for non-zero incident angle, the transmission is influenced by both even and odd resonances. Irregular frequency dependence of the transmission coefficient is typical for interference of two overlapping transmission bands [11, 12]. An overlap of two bands is confirmed also by the the change of the

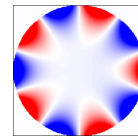


FIG. 7: Field H_z calculated at 5th resonance $f = 0.70564832$ in linear array of metallic cylinders ($R = 0.1a$).

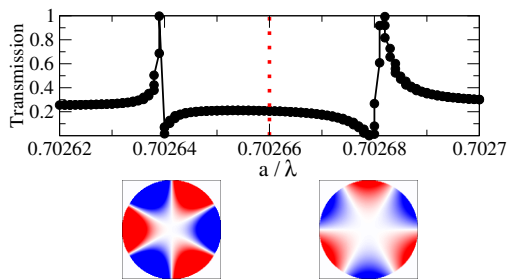


FIG. 8: Transmission coefficient of H_z polarized EM wave propagating through a linear chain of metallic cylinders calculated in the vicinity of the 3rd resonant frequency 0.70266. Spatial distribution of the magnetic field shown in the bottom panel confirms the even and odd symmetry of the lower ($a/\lambda = 0.702639$) and the upper ($a/\lambda = 0.702681$) Fano bands, respectively.

symmetry of electric field inside the cylinder when energy passes across the odd Fano band.

C. Thick Left-handed cylinders

Finally, we consider periodic array of cylinders made from left-handed material. with frequency dependent permittivity

$$\varepsilon(f) = 1 - \frac{1}{f^2} \quad (12)$$

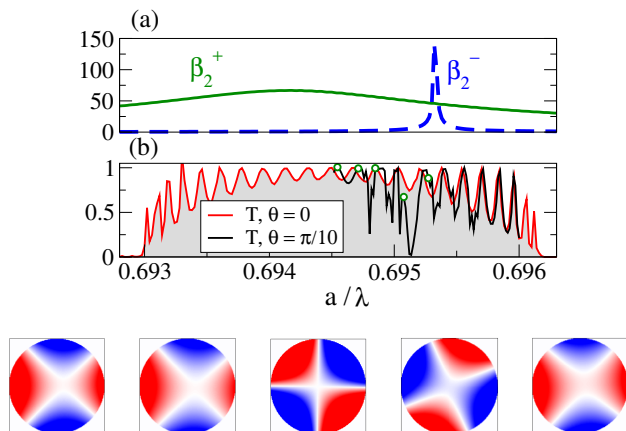


FIG. 9: (a) Resonant behavior of coefficients β_2^+ and β_2^- for the linear array of metallic cylinders. (b) Transmission coefficient for photonic slab made from $N = 24$ rows of metallic cylinders. While the odd resonance does not couple with perpendicularly incident plane wave, it affects strongly the transmission when the incident angle is $\theta = \pi/10$. Bottom panel shows the magnetic field H_z inside cylinders for frequencies $f = 0.694545, 0.694712, 0.694848, 0.695076$ and 0.695273 marked by green circles in panel (b). Note the change of the symmetry of the field when frequency passes the odd resonance.

and permeability

$$\mu(f) = 1 - 0.4 \frac{f^2}{f^2 - f_0^2} \quad (f_0 = 0.4). \quad (13)$$

In the frequency interval $0.4 < a/\lambda < 0.516$ cylinders behave as a left-handed material with both permittivity and permeability negative. In the analogy with theory of photonic crystals, one would expect that periodic array of such LH cylinders possesses standard band structure. However, negative values of permittivity and permeability allows also excitations of surface wave at the cylinder surface [18] in a similar way than on metallic rods.

Consider the E_z -polarized incident EM wave, with electric field parallel to the cylinder surface. It excites the TE polarized surface waves at the surface of the cylinder. The wavelength of surface wave λ_p is given by relation [27]

$$\frac{\Lambda_p}{a} = \frac{\lambda}{a} \sqrt{\frac{\mu^2 - 1}{\mu(\mu - \varepsilon)}} \quad (14)$$

Since Λ_p must be real, surface waves can be excited only in frequency intervals $f < f_{c1} = 0.416$ and $f > f_{c2} = 0.4473$. Therefore, similarly to the case of metallic rods, higher order Fano resonances are concentrated in the narrow frequency region where λ_p is small, namely for frequencies $f \rightarrow 0.4473^+$ where $\mu \rightarrow -1^-$.

Figure 10 shows coefficient α for resonances excited at isolated LH cylinder of radius $R = 0.45a$. A series of resonances converging to the frequency f_{c2} can be easily identified. Since $\mu \rightarrow -1$ when $f \rightarrow f_{c2}^+$, this series is equivalent to that discussed in ref. [17]. The structure

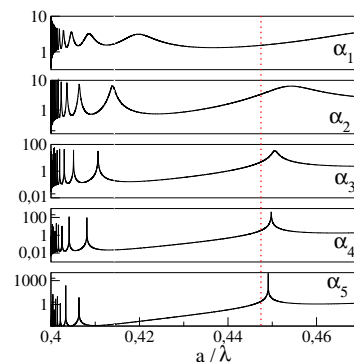


FIG. 10: Parameters α given by Eq. (1) for an isolated LH cylinder with permittivity and permeability given by Eqs. (12) and (13), respectively. Radius of cylinder $R = 0.45a$. Surface modes can be excited in two separated frequency interval: The upper interval starts at $f_{c2} = 0.4473$ (marked by red dotted line) where $\mu = -1$. In the lower interval $f < f_{c1}$, also a series of Fano resonances, similar to that excited in dielectrics are visible. Note that in contrast to dielectric and metallic rods, resonances appear in descending order: higher order resonances have smaller resonant frequency.

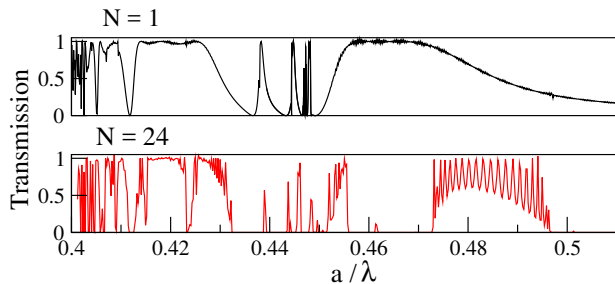


FIG. 11: Transmission of E_z polarized wave through $N = 1$ (top) and $N = 24$ (bottom) rows of LHM cylinders ($R = 0.45a$). Two intervals where Fano resonances are excited can be easily identified from irregular frequency dependence of the transmission coefficient.

of resonances in lower frequency interval reminds resonances on dielectric cylinders shown in Fig. 3. Note that the permeability μ diverges to negative infinite values when $f \rightarrow 0.4$. Interestingly, Fano resonances appear in the reverse order: higher resonances are excited for lower frequency [17].

Figure 11 shows the transmission coefficient of E_z -polarized wave propagating through linear array of LHM cylinders of radius $R = 0.45a$ and through a system of $N = 24$ rows of cylinders. For higher frequencies $f > 0.47$ as well as in the interval $0.41 < f < 0.44$ we observe transmission bands typical for dielectric photonic structures. In the frequency regions where Fano resonances are excited, we expect the existence of series of very narrow frequency bands. However, as shown in Fig. 12, identification of the order of the resonance is more difficult than in the case of metallic cylinders since the EM field inside the LH cylinder is given by a superposition of two or more overlapping resonant modes.

IV. CONCLUSION

Detailed analysis of spectra of Fano resonances is necessary for complete understanding of the frequency and transmission spectra of photonic structures. Resonances excited in simple structures – single cylinder, linear array

of cylinders – give rise to frequency bands in two dimensional structures. Such bands can overlap with periodic Bragg bands which causes various irregularities observed

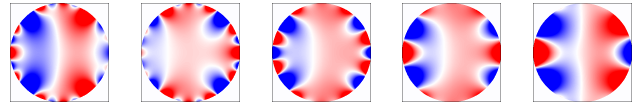


FIG. 12: Electric field E_z inside cylinders made from LH material. Frequency varies in narrow frequency interval between 0.44739 (left) to 0.448738 (right) i.e. slightly above the frequency f_{c2} .

in the transmission spectra of photonic crystals.

The spectrum of Fano resonances can be rather complicated: in dielectric cylinders, incident electromagnetic wave can excite a series of resonances for each symmetry of EM field. In contrast to dielectrics, metallic cylinder allows resonances associated with surface states. The richest spectrum of Fano resonances can be found in structures made from cylinders made from the left-handed material which combines properties of both dielectrics and metals.

Excitation of Fano resonances is associated with strongly inhomogeneous spatial distribution of electromagnetic fields in the photonic structure, especially when higher-order surface modes are excited. Numerical algorithms based either on the discretization of the space [29] or on the expansion of EM field into Fourier series [30] are therefore not appropriate for the analysis of such states. Our methods, based on the expansion of the electromagnetic field into cylinder eigenfunctions overcome this difficulty and is suitable for qualitative and quantitative analysis of photonic structures composed from elements with cylindrical symmetry.

Acknowledgment

This work was supported by the Slovak Research and Development Agency under the contract No. APVV-0108-11 and by the Agency VEGA under the contract No. 1/0372/13.

[1] U. Fano, *Effects of Configuration Interaction on Intensities and Phase Shifts*, Phys. Rev. **124**, 1866 (1961).
 [2] S. Fan, W. Suh and J. D. Joannopoulos, *Temporal couple-mode theory for the Fano resonance in optical resonators*, J. Opt. Soc. Am. A **20** 569 (2003).
 [3] S. Fan and J. D. Joannopoulos, *Analysis of guided resonances in photonic crystal slabs*, Phys. Rev. B **65** 235112 (2002).
 [4] V. N. Astratov, I. S. Culshaw, R. M. Stevenson, D. M. Whittaker, M. S. Skolnick, T. F. Krauss and R. M. De La Rue, *Resonant Coupling of Near-Infrared*

Radiation to Photonic Band Structure Waveguides, J. Light. Technol. **17**, 2050 (1999).
 [5] K. Ohtaka, H. Numata, *Multiple scattering effects in photon diffraction for an array of cylindrical dielectrics*, Phys. Lett. **73A**, 411 (1979).
 [6] A. E. Miroshnichenko *et al.*, *Fano resonances in nanoscale structures*, Rev. Mod. Phys. **82**, 2257 (2010).
 [7] B. Lukyanchuk *et al.*, *The Fano resonance in plasmonic nanostructures and metamaterials*, Nature Mat. **9**, 707 (2010).
 [8] A. N. Poddubny *et al.* *Fano interference governs wave*

- transport in disordered systems, Nat. Comm. **3**, 914 (2012).
- [9] M. V. Rybin, et al., *Mie scattering as a cascade of Fano resonances*, Optics Express **21**, 30107 (2013).
- [10] M. V. Rybin et al., *Phase diagram for transition from photonic crystals to dielectric metamaterials*, Nature Comm. **6**, 10102(1-6) (2015).
- [11] P. Markoš, *Fano resonances and bad structure of two dimensional photonic structures*, Phys. Rev. A **92** 043814 (2015).
- [12] K. Sakoda, *Optical Properties of Photonic Crystals*, Berlin, Heidelberg: Springer (2005).
- [13] J. D. Joannopoulos, S. G. Johnson, J. N. Winn and R. G. Meade, *Photonic Crystals: Molding the Flow of Light* 2nd edition. Princeton: Princeton University Press (2008).
- [14] K. Sakoda et al., *Photonic bands of metallic systems. I. Principle of calculation and accuracy*, Phys. Rev. B **64**, 045116 (2001);
T. Ito and K. Sakoda, *Photonic bands of metallic systems. II. Features of surface plasmon polaritons* Phys. Rev. B **64**, 045117 (2001).
- [15] E. Moreno et al., *Band structure computations of metallic photonic crystals with the multiple multipole method*, Phys. Rev. B **65**, 155120 (2001).
- [16] P. Markoš and V. Kuzmiak, *Coupling between Fano and Bragg bands in photonic band structure of two dimensional metallic photonic structures*, submitted (2016).
- [17] P. Markoš, *Guided modes in photonic structures with left-handed components*, Opt. Comm. **361** 65(2016).
- [18] R. Ruppin, *Surface polaritons of a left-handed medium*. Phys. Lett. A **277**, 61 (2000).
- [19] D. N. Natarov et al. *Effect of Periodicity in the Resonant Scattering of Light by Finite Sparse Configurations of Many Silver Nanowires*, Plasmonics **9**, 389 (2013).
- [20] A. A. Asatryan et al. , *Two-dimensional Green function and local density of states in photonic crystals consisting of a finite number of cylinders of infinite length*, Phys. Rev. E **63**, 046612 (2001);
A. A. Asatryan et al. *Local density of states of metamaterial photonic crystals* Australian Institute of Physics, 18th National Congress, (2008).
- [21] J. A. Stratton, *Electromagnetic Theory* New York: Mc Graw-Hill Comp., 1941.
- [22] H. C. van de Hulst, *Light scattering by small particles* Dover Publ. Inc, NY (1981).
- [23] M. Abramowitz and I. A. Stegun, *Handbook of Mathematical Functions* Dover Publ. (1965).
- [24] C. A. Pfeiffer, E. N. Economou and K. L. Ngai, *Surface polaritons in a circularly cylindrical interface: Surface plasmons* Phys. Rev. B **10**, 3038 (1974).
- [25] K. Sakoda, *Symmetry, degeneracy, and uncoupled modes in two-dimensional photonic lattices*, Phys. Rev. B **52**, 7982 (1995).
- [26] E. N. Economou, *Surface plasmons in thin films*. Phys. Rev. **182**, 539 (1969).
- [27] P. Markoš and Costas M. Soukoulis, *Wave Propagation: From Electrons to Photonic Crystals and Left-Handed Materials*, Princeton University Press, Princeton and Oxford, 2008.
- [28] Ali Soltani Vala et al. *Detailed study of flat bands appearing in metallic photonic crystals* Physica Status Solidi C **8**, 2965 (2011).
- [29] J. B. Pendry and A. MacKinnon, *Calculation of photon dispersion relations*, Phys. Rev. Lett. **69**, 2772 (1992).
P. Markoš and C. M. Soukoulis, *Numerical studies of left-handed materials and arrays of split ring resonators*, Physical Review E **65**, 036622 (2002).
- [30] J.J. Hench and Z. Strakoš, *The RCWA method - a case study with open questions and perspectives of algebraic computations*, Electron. Trans. Numer. Anal. **31**, 331, (2008);
G. Kajtár, *Electromagnetic properties of two dimensional periodic structures*, PhD Thesis, Bratislava (2014).